

## Quasi-Plasticity of $\text{Si}_3\text{N}_4$ -BN Composites

Kee Sung Lee, Seung Kun Lee\* and Do Kyung Kim

Dept. of Materials Science and Engineering, KAIST, Taejeon 305-701, Korea.

\*Materials Science and Engineering Laboratory, National Institute of Standards and Technology, Gaithersburg, MD20899, USA

질화규소-질화붕소 복합재료의 준소성 특성

이기성 · 이승전\* · 김도경

한국과학기술원 재료공학과

\*미국 표준과학연구소

(1997년 11월 14일 받음, 1997년 12월 22일 최종수정본 받음)

**초 록** 질화규소-질화붕소 복합재료의 접촉하중에 의한 손상거동을 질화붕소 첨가량의 함수로 고찰하였다. Indentation 응력-변형을 곡선은 선형성을 벗어나 소성 특성을 갖는 재료임이 밝혀졌으며, 재료 표면으로 부터의 ring이나 cone형상의 균열 대신 표면하부에 전단응력에 의한 마이크로 크기의 준소성 변형 영역이 넓게 형성되어 손상저항성이 높은 재료로의 활용이 기대되었다. 이 때 마이크로 파괴와 연관된 shear faults가 이 재료의 소성을 갖도록 하는데 중요한 역할을 하였다. 질화붕소의 첨가량이 증가함에 따라 질화규소-질화붕소 재료는 보다 soft해지고 준소성의 특성을 나타내었다.

**Abstract** The nature, degree, and evolution of contact damage from Hertzian contacts in silicon nitride-boron nitride composites( $\text{Si}_3\text{N}_4$ -BN) are investigated as a function of boron nitride content. The strong deviations of indentation stress-strain from elastic response indicate exceptional plasticity in  $\text{Si}_3\text{N}_4$ -BN. The absence of ring cracks or cone cracks on the surfaces is observed, indicating a high damage tolerance. Subsurface quasi-plastic deformation by shear stress is considerable and microdamage is widely distributed within the region below the contact. Shear faults associated with local microfailures play a precursor role in plasticity of this material. When boron nitride content increases,  $\text{Si}_3\text{N}_4$ -BN becomes softer and more quasi-plastic.

### 1. Introduction

Silicon nitride ( $\text{Si}_3\text{N}_4$ ) is a leading ceramic for structural applications because of its superior properties of toughness, strength, hardness, and chemical and thermal durability.<sup>1~4)</sup> Many structural applications such as cutting tools and bearings are subjected to severe contact stresses.<sup>3~4)</sup> However, conventional fine-grained silicon nitride is not damage tolerant and produces classical cone cracks outside the contact sites.<sup>5)</sup> One approach that has met with success in silicon nitride is to introduce large elongated grains by some in-situ processing route.<sup>5~6)</sup> This improved damage tolerance is attributed to crack bridging. Another way to improve damage tolerance is to introduce boron nitride (BN) as a second phase. BN with weak cleavage plane is an effective material in distributing the damage.<sup>7~8)</sup>

The Hertzian contact test with spherical indenters is simple and useful to investigate the nature of damage and quantify elastic and quasi-plastic properties in ceramics.<sup>5, 9~11)</sup> This test has also provides new insight into the micromechanics of contact damage. Several ceram-

ic systems, including silicon nitride, have been investigated by using this test. These studies revealed that the entire nature of the damage could be changed with modifications to the material microstructure, from a classical single cone fracture in fine-grained homogeneous ceramics to multiple subsurface microfracture in coarse-grained heterogeneous ceramics. Associated with this change in damage response is an increasing nonlinearity in the indentation stress-strain responses, a brittle-ductile transition. The brittle and ductile responses have radically different influences on strength loss and material removal properties of the material.

In this paper we investigated the nature, degree, and evolution of contact damage from Hertzian contacts in silicon nitride and boron nitride composites ( $\text{Si}_3\text{N}_4$ -BN). These materials were investigated as a function of boron nitride content. Especially, quasi-plasticity was quantified by nonlinearity of indentation stress-strain curve and material softness. We will demonstrate exceptional plasticity in this material with increasing BN content. Bonded-specimen technique was used to exam-

ine the nature of subsurface quasi-plastic damage.

## 2. Experimental Procedure

### 2.1. Sample preparation and characterization

Si<sub>3</sub>N<sub>4</sub>-BN composites were fabricated by common powder processing. BN powder was mixed with Si<sub>3</sub>N<sub>4</sub> powder mixtures during powder preparation. The Si<sub>3</sub>N<sub>4</sub> starting powder mixtures were  $\alpha$ -Si<sub>3</sub>N<sub>4</sub> (UBE-SN-E10, Ube Industries, Japan) with sintering additives of 2 wt% Al<sub>2</sub>O<sub>3</sub> (AKP50, Sumitomo Chemical Co. Ltd., Tokyo, Japan), 5 wt% Y<sub>2</sub>O<sub>3</sub> (H. C. Starck GmbH, Goslar, Germany) and 1 wt% MgO (High Purity, Baikowski Co., NC, U.S.A.). BN (Aldrich Chemical, Milwaukee, WI, U.S.A.) content was varied from 5 to 30 wt%. Each powder batch was ball milled using alumina balls in isopropanol for 24 hr. After milling, the slurries were dried in the oven and sieved to form granulated powder. The resulting powder mixtures were hot pressed at 1730°C under 30 MPa for 1 hr.

Each specimen was cut and the surface was polished to 1 $\mu$ m, and plasma etching was performed in CF<sub>4</sub> and O<sub>2</sub> gas for 10 min to reveal grain structures. Microstructural examination was carried out by scanning electron microscopy (SEM). Sintered densities of specimens were measured by the Archimedes principle.

A routine Vickers test was performed to evaluate individual material property. Hardness and toughness were calculated by measuring the projected impression area and crack lengths at the contact load. Hardness was calculated by the following equation<sup>12)</sup>:

$$H = P/2a^2 \quad (1)$$

where,  $P$  is load and  $a$  is the average value of half-diagonal lengths. Indentation crack length,  $c$ , was used to calculate the toughness,  $T_0$ , using the following equation<sup>13)</sup>:

$$T_0 = \chi P/c^{3/2} \quad (2)$$

where,  $P$  is the indentation load, and  $\chi = 0.016 (E/H)^{1/2}$  with  $E$ , elastic modulus and  $H$ , the indentation hardness.

### 2.2. Hertzian indentation

Hertzian indentations were made on polished surfaces of Si<sub>3</sub>N<sub>4</sub>-BN composites. First, a test was made to determine indentation stress-strain curves.<sup>11)</sup> Test surfaces were gold coated before indentation to facilitate measurement of contact radius  $a$ . Then, we evaluated the

indentation stress and strain. Measurements of contact radius  $a$ , sphere radius  $r$  and indentation load  $P$  enable us to evaluate

$$\text{Indentation stress } p_0 = P/\pi a^2 \quad (3)$$

$$\text{Indentation strain } a/r \quad (4)$$

The spherical indenters were used with tungsten carbide spheres, radius of 1.98~12.7 mm at loads up to  $P = 4000$  N. The elastic modulus was determined from the initial slope in the elastic region of indentation stress-strain curve. Indentations were also made on each composite to determine critical loads for yield  $P_Y$  by first residual impressions, and then yield stress  $Y$ , from  $p_Y = P_Y/\pi a^2 = 1.1Y$ .

We used bonded-interface specimen configuration to investigate subsurface damage. The same polished bars (3 mm  $\times$  4 mm  $\times$  25 mm) were clamped each other with a thin layer ( $\leq 10\mu$ m) of adhesive. The surface was then ground and polished perpendicular to the bonded interface. As we can see in Fig. 1, the indentations were made symmetrically across the interface at  $P = 2000$  N using WC spheres of radius  $r = 1.98$  mm. After indentation, the two bars were separated by dissolving the glue in acetone, and viewed optically in Nomarski illumination.

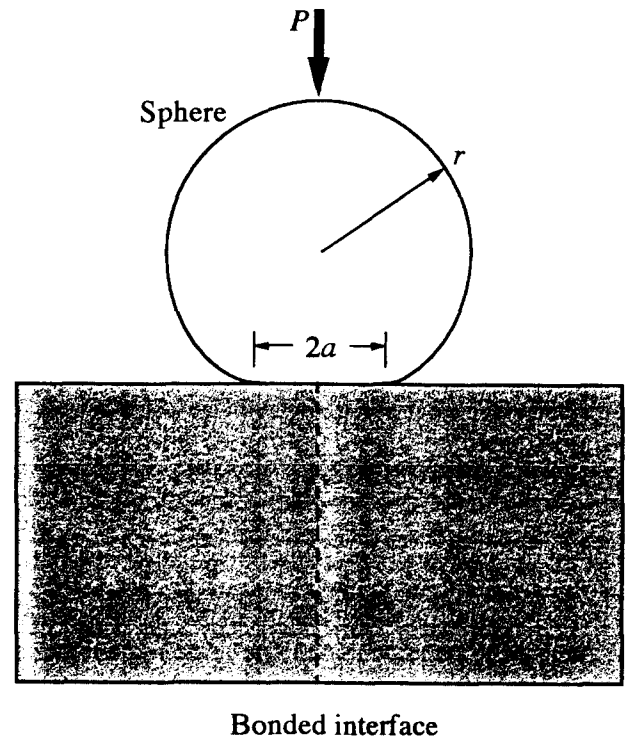


Fig. 1. Schematic diagram of Hertzian indentation.

### 3. Results and Discussion

#### 3.1. Material characterization

Figure 2 shows the representative SEM micrograph of the polished specimen, 20 wt% BN added composites, relatively isotropic in  $\text{Si}_3\text{N}_4$  and anisotropic in BN grains. The microstructure of matrix,  $\text{Si}_3\text{N}_4$  material, shows a typical microstructure with elongated  $\beta$ - $\text{Si}_3\text{N}_4$  grains. The dark phase indicates the BN site because BN grains are evaporated during the plasma etching process. The microstructure shows well-distributed BN platelets with 1.5 ~ 6  $\mu\text{m}$  diameter and 0.2 ~ 0.6  $\mu\text{m}$  thickness. Note the aligned direction of BN platelets. Most platelets were aligned in a parallel direction to the surface, normal to hot press direction. This is due to the rearrangement of platelets during hot pressing. Full density was confirmed using the Archimedes method. The porosity level was less than  $\leq 0.1\%$  regardless of the BN additive content.

The hardness variation with the BN content is shown in Fig. 3. As the BN content increased, the hardness decreased linearly. The hardness values of 30 wt% BN added  $\text{Si}_3\text{N}_4$  composites were less than a third of hardness of  $\text{Si}_3\text{N}_4$  matrix, indicating a softening effect of the BN additives.

Although the hardness was not affected by anisotropic BN structure, the toughness results showed a strong influence of anisotropy as shown in Fig. 4. Note the difference in toughness in Fig. 4 between parallel and normal to hot press direction. The difference increased with increasing BN content in  $\text{Si}_3\text{N}_4$  matrix. Anisotropy in toughness resulted from the anisotropic microstructure of this system. Irrespective of BN composition, the cracks parallel to hot press direction are mostly sup-

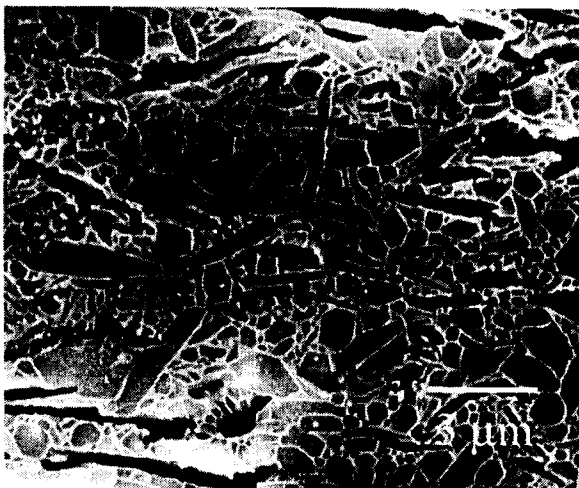


Fig. 2. SEM micrograph of  $\text{Si}_3\text{N}_4$ -20wt%BN composite.

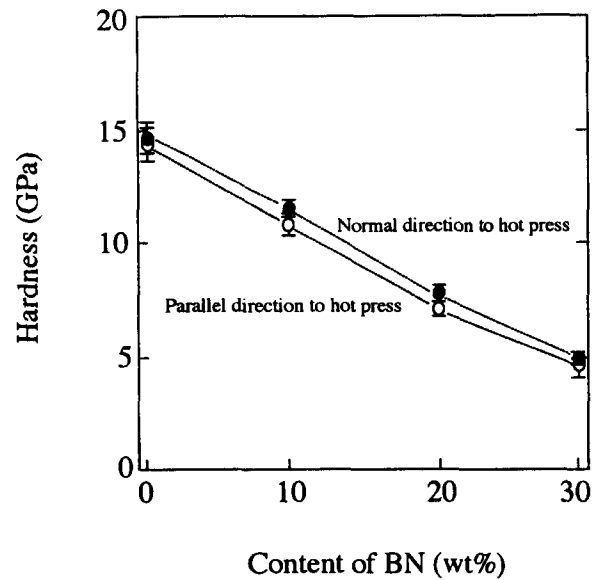


Fig. 3. Hardness of Vickers-indented  $\text{Si}_3\text{N}_4$ -BN composites as a function of BN content.

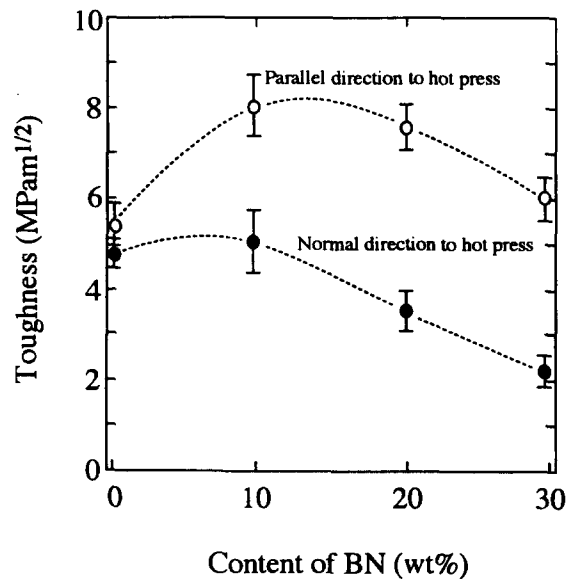


Fig. 4. Toughness of Vickers-indented  $\text{Si}_3\text{N}_4$ -BN composites as a function of BN content.

pressed as shown in Fig. 5. The cracks propagate mostly in normal direction to hot press. The maximum fracture toughness was about 8  $\text{MPam}^{1/2}$  at 10wt% BN added composites in parallel direction to hot press. Thereafter, the toughness was decreased by the weakness of BN.

#### 3.2. Hertzian indentation

"Quasi-plastic" behavior can be observed by Hertzian indentation technique.<sup>9,11)</sup> Whenever the material includes weak interfaces and elongated large grains, they show damage accumulation without cone crack. A region beneath the spherical indenter is deformed by the shear stress, but this deformation is completely differ-

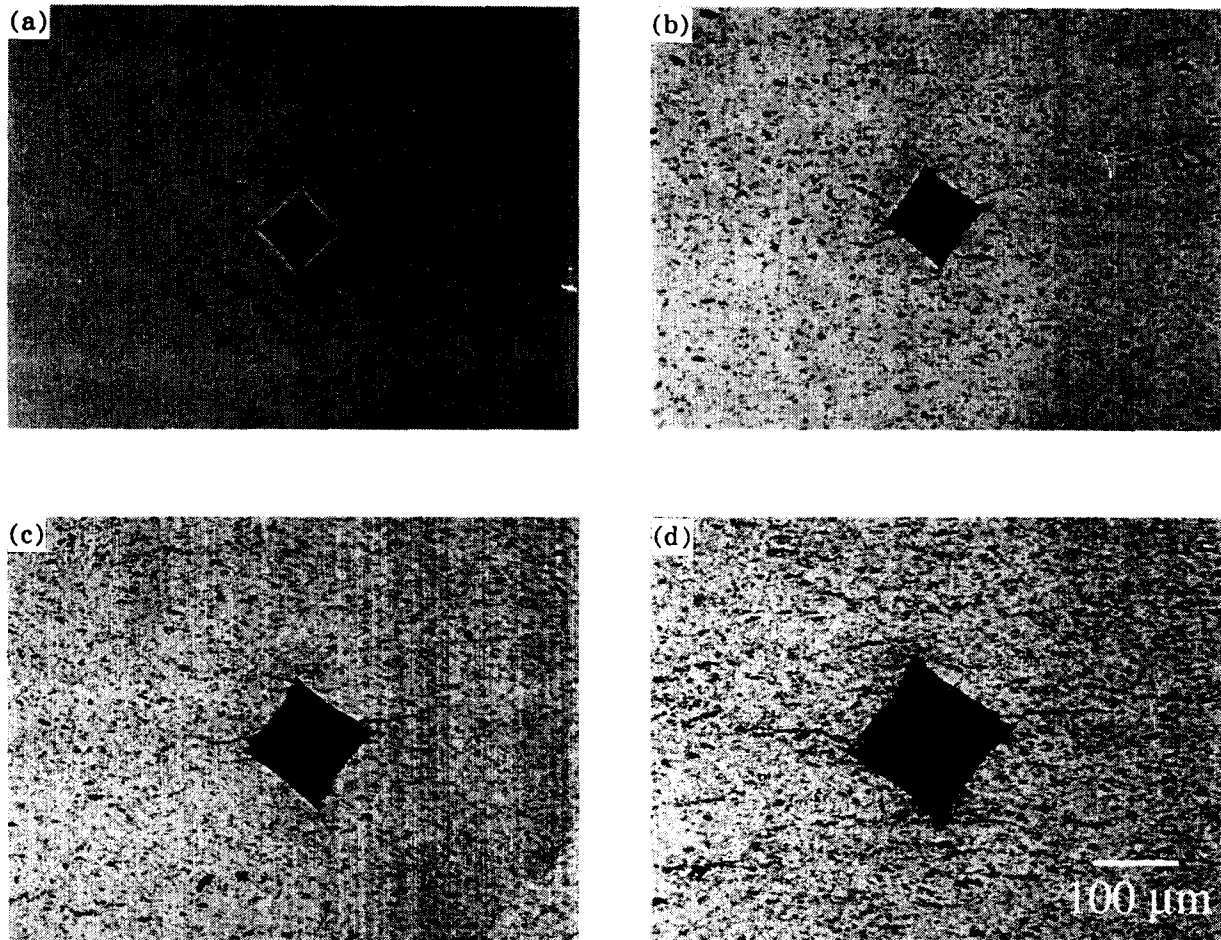


Fig. 5. Micrographs of Vickers indentation cracks under load = 10 kgf in (a)  $\text{Si}_3\text{N}_4$ , (b)  $\text{Si}_3\text{N}_4$ -10wt%BN, (c)  $\text{Si}_3\text{N}_4$ -20wt%BN, and (d)  $\text{Si}_3\text{N}_4$ -30wt%BN.

ent from a deformation of metal. This deformation is related to the microstructure of ceramic material because control of “brittle to quasi-plastic” behavior is activated by incorporation of weak interfaces, large and elongated grains. This behavior is very important because it is expected as a damage absorbent materials. Instead of a discrete macroscopic cone crack, a diffuse micro-fractured damage zone is developed beneath the indenter for ceramic material with heterogeneous microstructure. So far this behavior was evaluated by the slope of the plastic region in indentation stress-strain curves. When this slope is relatively low, the material is said to have more “quasi-plastic” behavior. Generally, the nonlinearity of the indentation stress-strain curve shows effective quasi-plasticity. The contact becomes inelastic only if indentation stress exceeds some critical value, yield stress  $P_y$ , where irreversible deformation can be developed.

Figure 6 shows indentation stress-strain curves for  $\text{Si}_3\text{N}_4$ -BN composites. The  $\text{Si}_3\text{N}_4$  matrix is close to the linearity, but as the BN content increases, the indenta-

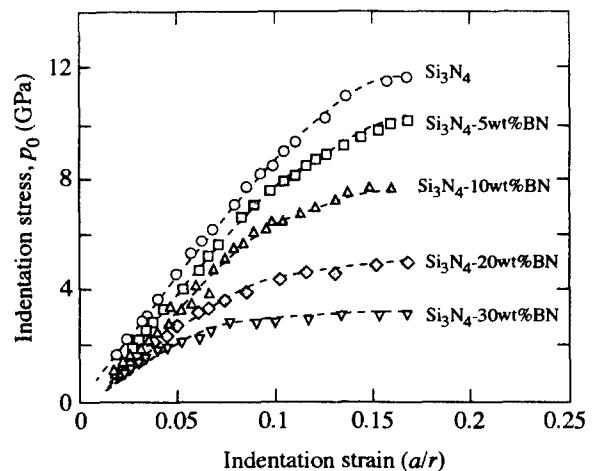
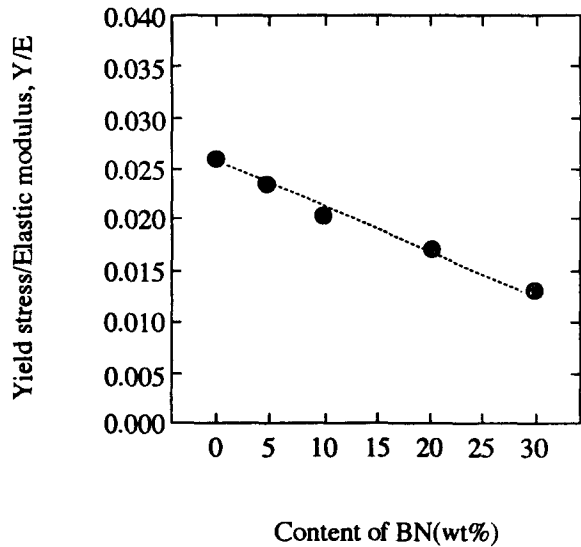


Fig. 6. Indentation stress-strain curves for  $\text{Si}_3\text{N}_4$  and  $\text{Si}_3\text{N}_4$ -BN composites from Hertzian contact tests.

tion stress-strain curves shift downward because elastic modulus and yield stress decrease. This indicates that composite material becomes “soft”, so ultimately shows “quasi-plastic” behavior. Elastic modulus,  $E$  and yield stress,  $Y$  can be determined using these indenta-

Table 1. Properties of elastic modulus and yield stress.

Material	Young's modulus (GPa)	Yield stress (GPa)
Si <sub>3</sub> N <sub>4</sub>	320	8.4
Si <sub>3</sub> N <sub>4</sub> -5wt%BN	278	6.7
Si <sub>3</sub> N <sub>4</sub> -10wt%BN	222	4.5
Si <sub>3</sub> N <sub>4</sub> -20wt%BN	160	2.8
Si <sub>3</sub> N <sub>4</sub> -30wt%BN	119	1.6

Fig. 7. The ratio of yield stress and elastic modulus of Si<sub>3</sub>N<sub>4</sub>-BN composites as a function of BN content.

tion stress-strain curves. The value of  $E$  is obtained from the initial slope, and  $Y$  is measured from the load corresponding to the first detection of residual impression. The values of  $E$  and  $Y$  of each composite are shown in Table 1. The elastic modulus values shown in Table 1 decrease with an increasing BN content by about a factor of three in 30 wt% BN added composite. In comparison, the yield stress values decrease by more than a factor of three. This result indicates that the composite becomes softer when the BN content increases. In metal,  $Y/E$  is a good parameter to indicate the softness of material. For soft metals (low  $Y/E$ ), plasticity dominates and the displaced material piles up around the indenter. The indentation stress-strain curve flattens out beyond the yield point.<sup>14)</sup> The replotted  $Y/E$  as a function of BN content is shown in Fig. 7. The fact that the  $Y/E$  ratio decreases when the BN content increases shows this composite is softened further by the addition of BN.

Figure 8 illustrates section views of contact damage formed at load  $P=2000$  N using a WC ball with a radius of 1.98 mm. This contact damage was formed by using the indentation technique as shown in Fig. 1. In

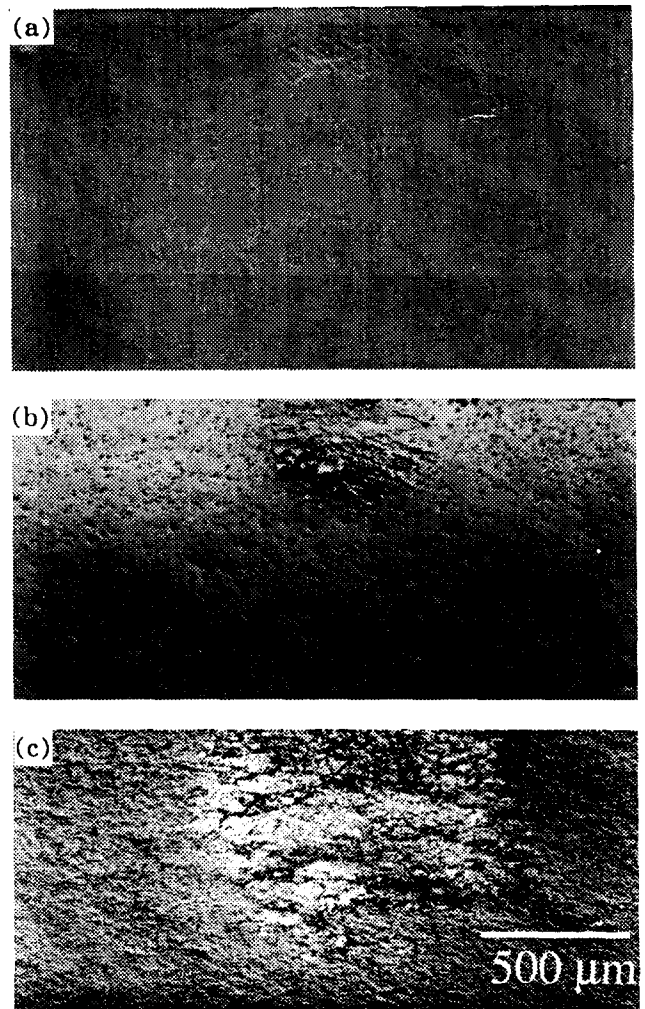
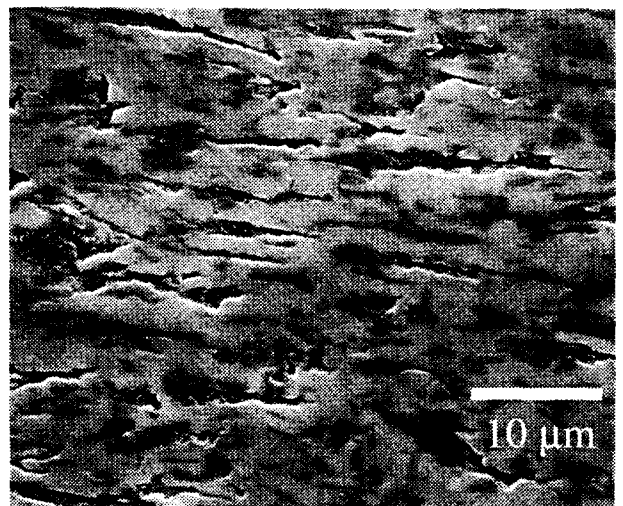
Fig. 8. Side views of Hertzian contact damage in (a) fine-grained monolithic Si<sub>3</sub>N<sub>4</sub>, (b) Si<sub>3</sub>N<sub>4</sub>-5wt%BN and (c) Si<sub>3</sub>N<sub>4</sub>-30wt%BN, from WC sphere with radius  $r=1.98$ mm at load  $P=2000$ N.

Fig. 9. SEM micrograph from center region of section damage zone from Fig. 8(c). Microfailures at interphase boundaries are evident.

monolithic Si<sub>3</sub>N<sub>4</sub>, a cone crack is formed in the vicinity of the contact point, confirming brittleness and high

flaw sensitivity. However, when the BN content increases, the "quasi-plastic" behavior increases and the subsurface plasticity zone beneath the contact expands substantially. This evolution of the damage accumulation is clearer when the BN content increases. The "quasi-plastic zone" is fully developed in 30wt%BN added Si<sub>3</sub>N<sub>4</sub> composites. This is due to the micro-short crack formation by maximum shear stress. Figure 9 shows the enlarged SEM micrograph of the "quasi-plastic zone". The micrograph shows that the nature of the damage consists of microcrack and shear fault formation by grain sliding along the weak cleavage or boundaries.

#### 4. Conclusion

The fact that the plasticity of ceramic can be increased on a micro-scale was revealed by the evaluation of indentation stress-strain curve of Si<sub>3</sub>N<sub>4</sub>-BN composites. When the amount of BN increased in Si<sub>3</sub>N<sub>4</sub>-BN composites, the indentation stress-strain curve deviated the linearity by its "quasi-plastic" behavior. We confirmed that this behavior comes from the low hardness, low elastic modulus, low yield stress, and ultimately, high softness of composites.

Extensive damage distribution was found in these composites with cone crack suppression in the Hertzian indentation test; therefore, these materials can be used as damage absorbent materials, and it was ascertained that "quasi-plastic" behavior is a very important parameter in developing damage tolerant material.

#### Acknowledgement

We acknowledge B. R. Lawn in NIST for his encouragement and support in this research.

#### References

1. F. F. Lange, *J. Am. Ceram. Soc.*, **59**(10) 518 (1973)
2. G. Himsolt, H. Knoch, H. Huebner and F. W. Kleinlein, *J. Am. Ceram. Soc.*, **62**(1-2) 29 (1979)
3. R. Nathan Katz, *Materials Research Society Symposium Proceedings*, **287** 197 (1992)
4. D. W. Recherson and P. M. Stephan, *Materials Science Forum*, **47** 282 (1989)
5. S. K. Lee, S. Wuttiphon and B. R. Lawn, *J. Am. Ceram. Soc.*, **80**(9) 2367 (1997)
6. C.-W. Li, S.-C. Lui and J. Goldacker, *J. Am. Ceram. Soc.*, **78**(10) 2619 (1995)
7. E. H. Lutz and M. V. Swain, *J. Am. Ceram. Soc.*, **75**(1) 67 (1992)
8. S. Baskaran, S. D. Nunn, D. Popovic, and J. W. Halloran, *J. Am. Ceram. Soc.*, **76**(9) 2209 (1993)
9. B. R. Lawn, N. P. Padture, H. Cai, and F. Guiberteau, *Science*, **263** 1114 (1994)
10. A. C. Fischer-Cripps and B. R. Lawn, *Acta mater.*, **44**(2) 519 (1996)
11. F. Guiberteau, N. P. Padture, H. Cai and B. R. Lawn, *Phil. Mag. A*, **68**(5) 1003 (1993)
12. D. Tabor, *Hardness of Metals*, Clarendon, Oxford, (1951)
13. D. B. Marshall, T. Noma, and A. G. Evans, *J. Am. Ceram. Soc.*, **65**(10) C175 (1982)
14. A. C. Fischer-Cripps and B. R. Lawn, *J. Am. Ceram. Soc.*, **79**(10) 2609 (1996)